Characterization of neuromas in peripheral nerves and their effects on heterotopic bone formation

Jordan Minarelli[1], Eleanor L Davis[1], Austin Dickerson[1],
William C Moore[1], Julio A Mejia[1], Zbigniew Gugala[2],
Elizabeth A Olmsted-Davis[1,3,4], and Alan R Davis[1,3,4]

Abstract

The formation of neuromas involves expansion of the cellular components of peripheral nerves. The onset of these disorganized tumors involves activation of sensory nerves and neuroinflammation. Particularly problematic in neuroma is arborization of axons leading to extreme, neuropathic pain. The most common sites for neuroma are the ends of transected nerves following injury; however, this rodent model does not reliably result in neuroma formation. In this study, we established a rodent model of neuroma in which the sciatic nerve was loosely ligated with two chromic gut sutures. This model formed neuromas reliably ($\sim$95%), presumably through activation of the neural inflammatory cascade. Resulting neuromas had a disorganized structure and a significant number of replicating cells. Quantification of changes in perineurial and Schwann cells showed a significant increase in these populations. Immunohistochemical analysis showed the presence of β-tubulin 3 in the rapidly expanding nerve and a decrease in neurofilament heavy chain compared to the normal nerve, suggesting the axons forming a disorganized structure. Measurement of the permeability of the blood–nerve barrier shows that it opened almost immediately and remained open as long as 10 days. Studies using an antagonist of the β3-adrenergic receptor (L-748,337) or cromolyn showed a significant reduction in tumor size and cell expansion as determined by flow cytometry, with an improvement in the animal's gait detected using a Catwalk system. Previous studies in our laboratory have shown that heterotopic ossification is also a result of the activation of neuroinflammation. Since heterotopic ossification and neuroma often occur together in amputees, they were induced in the same limbs of the study animals. More heterotopic bone was formed in animals with neuromas as compared to those without. These data collectively suggest that perturbation of early neuroinflammation with compounds such as L-748,337 and cromolyn may reduce formation of neuromas.

Introduction

Neuroma results from a disorganized non-neoplastic growth of cells associated with peripheral nerves leading to the formation of a benign tumor. These are often associated with nerve injury, such as crush, stretch, or transection, and exhibit axonal extension and potential arborization.[1,2] In many cases, the blood–nerve barrier (BNB) is disrupted due to the disorganized cellular expansion eliminating essential protection of the axons from the external environment. Thus, neuroma can often lead to allodynia or an increased response of nerves and

[1]Center for Cell and Gene Therapy, Baylor College of Medicine, Texas Children's Hospital and Houston Methodist Hospital, Houston, TX, USA
[2]Department of Orthopedic Surgery and Rehabilitation, University of Texas Medical Branch, Galveston, TX, USA
[3]Department of Pediatrics – Section Hematology/Oncology, Baylor College of Medicine, Houston, TX, USA
[4]Department of Orthopedic Surgery, Baylor College of Medicine, Houston, TX, USA

Corresponding Author:
Elizabeth A Olmsted-Davis, Baylor College of Medicine, One Baylor Plaza, N1010, Houston, TX 77030, USA.
Email: edavis@bcm.edu

pain sensitization, causing a pain response from stimuli that normally do not provoke pain.[3] Often, neuromas associated with disease have been further characterized as to the type of cell that has expanded, such as Schwannoma is a neuroma derived from expansion and disorganization of Schwann cells. One of the most common neuromas in humans is Morton's neuroma of the foot, which arises from the disorganized expansion of perineurial cells.[4] Although the exact causes of this neuroma are unknown, the data suggest that a slight malformation of the foot, leading to changes in biomechanics of walking, may cause chronic pressure on the nerve, leading to injury.[5,6]

Although neuromas are often painful, in some cases the pain can be extreme, leading to significant loss of function for the patient and limiting motion in the affected area.[7] These painful neuromas are more common after amputation.[8] Currently, antipsychotic or anti-seizure medications are the only nonsurgical treatment option, but these generally will not resolve the neuroma but rather provide some relief.[9,10] Surgical resection of the nerve particularly in the amputation stump can provide benefit, and it requires that the nerve end be placed in muscle or bone to limit a direct stimulation (from pressure or contact) during normal activities[8] and a chance to connect with another nerve.

Heterotopic ossification (HO), bone formation at a *de novo*, non-skeletal site, also commonly occurs in the amputation stump. Recent studies of HO show a correlation between substance P release and the activation of sensory nerves.[11–13] Upon induction of HO, mast cells appear to recruit to sensory nerves, leading to release of pain mediators, substance P, and calcitonin gene-related peptide.[14] This establishes the initial steps of neuroinflammation.[12] During neuroinflammatory phase, substance P release can recruit mast cells to the nerve and, upon their degranulation, lead to further activation of the nociceptor signaling. Surprisingly, these early steps lead to the activation of the sympathetic nervous system and result in the proliferation of perineurial fibroblasts.[15] These proliferating perineurial fibroblasts express the β3-adrenergic receptor (ADRβ3) and are present in the tissues surrounding the new bone formation.[15] Cromolyn is a drug previously shown to block neuroinflammation by inhibiting mast cell degranulation.[12] Administration of cromolyn has been shown to significantly decrease or prevent HO.[12] However, the ability of cromolyn to block neuroma formation has not been investigated.

Here, we established a rat model of neuroma where tumors reliably form in 10 days after loose ligation of the sciatic nerve with chromic gut suture. Characterization of this model reveals that perineurial cells expand rapidly, while the BNB is compromised. Two compounds,

cromolyn and an ADRβ3 antagonist (L-748,337), were tested to determine if they can suppress neuroma formation in this model. In these studies, expansion of the cellular component of peripheral nerves was characterized by flow cytometry in the presence of these compounds. Functional recovery analysis was also performed using a Catwalk system to determine if these compounds reduced neuroma-related pain and improved gait. Finally, because neuromas and HO often occur simultaneously in amputation stumps, studies were performed to identify whether they could influence each other.

Materials and methods

Induction of neuroma

Neuromas were formed in Wistar rats and C57BL/6 mice (Jackson Laboratory, Bar Harbor, ME) by placing four chromic gut sutures, 2–0 816H or 4–0 635H, respectively (Ethicon, Somerville, NJ) around the sciatic nerve. The nerve was exposed, and two adjacent suture loops were loosely run around the nerve and tied on each side of a gap of approximately 3 mm (Figure 1(a)). Ten days after the induction of neuroma, animals were euthanized and whole hind limb tissue or isolated sciatic nerves were harvested and either sucrose-fixed, fixed in formalin, or snap frozen. The timeframe was selected based on identifying the earliest period at which 95% or greater of the animals would possess neuroma.

All animal studies were conducted under an Institutional Animal Use and Care Committee approved protocol in accordance with Organization of Laboratory Animal Welfare. All animals were housed in an Assessment and Accreditation of Laboratory Animal Care accredited vivarium under standard conditions as described by Office of Laboratory Animal Welfare. Animals were randomly selected based on age and health. Experimental groups were randomly selected and animals coded to avoid bias. Both genders were analyzed and no differences observed. Group sizes are based on historical data; however, power analysis was repeated after data collection to ensure appropriate group sizes.

Evans blue dye

Ten days after induction of neuroma in Wistar rats, animals were systemically injected with 2% Evans blue dye as previously described.[16] One hour after injection, animals were euthanized, and a 5 mm section of the sciatic nerve was isolated. Nerve sections were placed in formamide at 65°C as described by Beggs et al.[16] in order to extract the blue dye from the
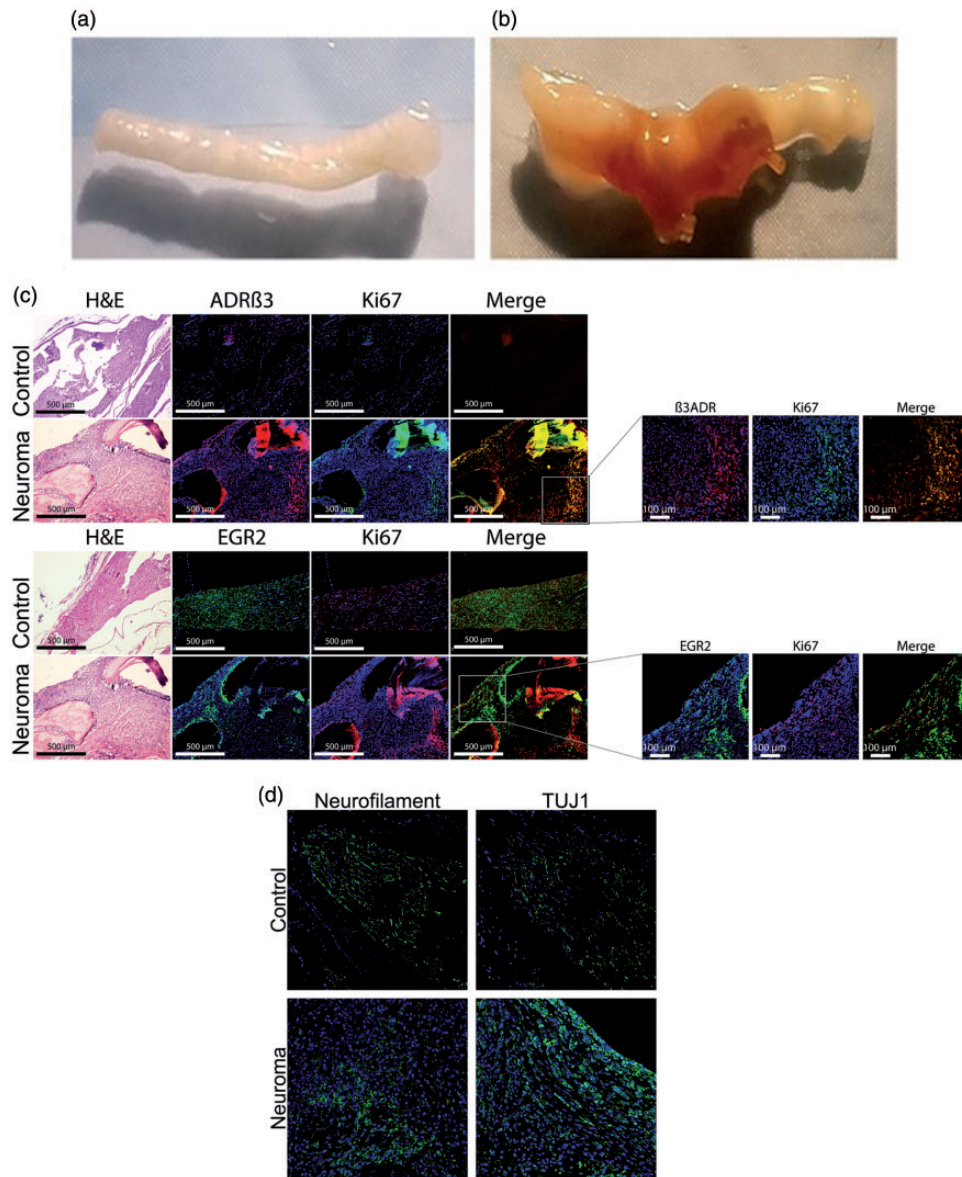
Figure 1. (a) and (b) Representative photographs of a (a) normal rat sciatic nerve and (b) a rat sciatic nerve 10 days after introduction of two chromic gut sutures loosely ligated around the sciatic nerve at approximately 3 mm apart. Arrows indicate the nerve structure and neuroma formed. (c) and (d) Representative photomicrographs of rat sciatic nerve or a rat sciatic nerve containing a neuroma. (c) Perineurial cell expansion was determined by immunostaining for ADRβ3 (red) and Ki-67 (green) which detects replicating cells. Schwann cells were identified using EGR2 (green) and proliferation was confirmed using Ki-67 (red). In all cases, tissues were counterstained with DAPI (blue) to detect nuclei. Images were generated using fluorescence microscopy, and scale bars are as indicated. Low magnification images allowed for orientation of the cells in the nerve/neuroma structure. Small insets have been magnified to show coexpression of markers. Serial sections were stained with hematoxylin and eosin (H&E) stain for tissue visualization. (d) Serial sections have been immunostained for neurofilament (green) and β-tubulin 3 (TUJ1, green) to determine changes in axons; ADRβ3: β3-adrenergic receptor.

nerve.[16] The dye concentration was then determined by spectrophotometry.

Cell culture

A primary skin fibroblast cell line was created from skin biopsies of a Wistar rat (Wistar skin fibroblast, WSF).

Cells were propagated in a humidified incubator at 37°C temperature under 5% CO_2 atmosphere in Dulbecco's modified Eagle's medium (Sigma, St. Louis, MO) supplemented with 10% fetal bovine serum (HyClone, Logan, UT), 100,000 U/L penicillin, 100 mg/L streptomycin, and 0.25 mg/L amphotericin B (Invitrogen Life Technologies, Gaithersburg, MD).

BMP2 delivery in vivo

Replication defective E1-E3 deleted human type 5 adenovirus possessing cDNA for bone morphogenetic protein 2 (BMP2) (AdBMP2) or no transgene (AdEmpty) in region E1 were constructed as previously described.[17] Mouse skin fibroblasts or WSF were transduced at 5000 virus particles per cell with 0.75% GeneJammer to achieve greater than 90% transduction efficiency as previously described.[18] All adenoviruses were negative for replication competent adenovirus. AdBMP2 transduced cells expressed approximately 20 ng/ml/ 5×10^6 cells.

Transduced cells were resuspended in 0.1 ml of phosphate-buffered saline (PBS) and delivered by intramuscular injection into the quadricep muscle of C57BL/6 mice or Wistar rats. After euthanasia, hind limbs were harvested and either sucrose-fixed, fixed in formalin, or snap frozen.

Cromolyn and L-748,337 treatment

Cromolyn (Alfa Aesar, Ward Hill, MA) was suspended in pharmaceutical grade saline (100 mg/mL) and delivered via an intraperitoneal injection to C57BL/6 mice or Wistar rats (150 mg/kg) daily for 10 days. L-748,337 (Santa Cruz Biotechnology, Inc., Dallas, TX) was suspended in pharmaceutical grade saline (1.0 mg/mL) and delivered via an intraperitoneal injection to C57BL/6 mice or Wistar rats (1.2 mg/kg) daily for 10 days. Control animals received 100 µl of pharmaceutical grade saline.

Gate analysis

Animals were subjected to gait analysis using the CatWalk Automated Gait Analysis System (Noldus Information Technology, Leesburg, VA) and software version XT 9.1. Gait analysis was performed in mice pre-operatively (baseline) as well as 5 and 10 days after surgery. Each animal completed three runs (n = 3).[19] Compliant runs for each animal were set for a maximum time of 10 seconds necessary to complete a defined path length, with a maximum variation in speed up to 60%.

Flow cytometry and fluorescence-activated cell sorting

The cells from hind limb tissues were isolated and collagenase digested as previously described.[15] Fluorescence-activated cell sorting (FACS) was performed using a fluorochrome-labeled antibody against the ADRβ3 using a FACS Aria II cell sorter (BD Biosciences, San Jose, CA) equipped with analyzing software (BD FACSDiva software version 8.0.1, BD Biosciences).

Tissue processing

Hind limbs were harvested from the animals and decalcified (Richard-Allan Scientific Decalcifying solution, Cat No.: 8340–1, Thermo Fisher Scientific, Waltham, MA). Following decalcification, the tissues were fixed with 4% paraformaldehyde. Tissues were processed and embedded in paraffin. All tissues were serially sectioned in 5 µm sections in a cryostat. Hematoxylin and eosin staining was performed on every 10th slide.

Immunohistochemistry

Immunohistochemistry was conducted as previously described by Olmsted-Davis et al.[20] Primary antibodies were used at a dilution of 1:100–1:200 and secondary antibodies (Alexa Fluor 488, 594, or 647; Invitrogen Life Technologies, Carlsbad, CA) at a 1:500 dilution. Primary antibodies used were as follows: rabbit polyclonal antibodies (ADBR3) (Abcam, Cambridge, UK), Ki67 (Abcam, Cambridge, UK), early growth response protein 2 (EGR2) (Proteintech Group, Inc., Rosemont, IL) and mouse monoclonal antibodies beta 3 tubulin (TUJ1) (Promega, Madison, WI), and neurofilament 1 (NF1) (Sigma-Aldrich, St. Louis, MO). Primary and secondary antibodies were diluted in PBS with 2% bovine serum albumin. Tissues were counterstained and covered with Vectashield mounting medium containing 4′,6-diamidino-2-phenylindole (DAPI) (Vector Laboratories, Burlingame, CA). Stained tissue sections were examined using an Olympus BX41 microscope (Olympus Corporation of the Americas, Waltham, MA) equipped with a reflected fluorescence system, using a $10 \times /0.40$ numerical aperture objective lens. Stained tissue sections shown in Figure 1(d) were examined by confocal microscopy (Zeiss Inc, Thornwood, NY, LSM 780). To ensure signal specificity, controls were performed, and the specific absorption spectrum from each primary–secondary pair was captured. Lambda mode was then used to separate signal into each component. In this way, autofluorescence was filtered out.

Microcomputed tomography

MicroCT scans of the whole hind limb specimens were performed at 9.3 µm spatial resolution (SkyScan 1174; Micro Photonics Inc, Allentown, PA). Regions of interest were defined for each specimen to isolate the new mineralized tissue formed within the skeletal musculature at the injection site. The volume of heterotopic bone was calculated using CTAn software package (Micro Photonics Inc, Allentown, PA) with a density threshold set at 0.2 g/cm^3. Bone mineral density of the heterotopic bone was assessed following a scan of hydroxyapatite phantoms to establish the attenuation coefficients at 0.25 and 0.75 densities. The 3D

microCT reconstructions were created using CTVox software package (Micro Photonics Inc, Allentown, PA).

Statistical analysis

A one-way analysis of variance with a Tukey's post hoc correction for multiple comparisons with a 95% confidence interval (p < 0.05) was used for comparisons between treatment groups.

Results

Characterization of neuroma

Neuromas were formed by placing two loose ligations around the rat sciatic nerve after surgical exposure using chromic acid-treated suture (chromic gut) (Figure 1(a)). This model reliably (90%–95%) formed neuromas between the two sets of looped sutures in a minimum of 10 days (Figure 1(a) and (b)). Neuroma formation was assessed with respect to control sciatic nerves that were surgically exposed but not ligated with the suture. Isolated neuromas were analyzed using immunohistochemistry to determine the types of cells contributing to the neuroma. A subset of disorganized cells was observed to be expressing the ADRβ3 in the neuroma (Figure 1(c), panel a). This marker was selected because we have previously demonstrated its presence on replicating perineurial cells in peripheral nerves during the early stages of HO.[15] The majority of these ADRβ3 perineurial cells were found to be proliferating as indicated by positive immunostaining with the Ki67 antibody (Figure 1(c)). These cells were not present in the control nerve (Figure 1(b)). EGR2 also known as Krox20, a marker of Schwann cells, is present in both the control and neuroma (Figure 1(b)). However, similar to the ADRβ3⁺ cells, the EGR2⁺ cells appear disorganized and a subpopulation is replicating (Figure 1(b), panel b) in the neuroma.

Alternatively, while EGR2 expression is present, many of these cells are not replicating. Counting of the staining of every fifth slide costained for EGR2 and ADRβ3 throughout the neuroma suggests that there are more ADRβ3⁺-expressing cells than EGR2. Since axonal expansion is a hallmark of neuromas, we next analyzed for changes in NF. Similar to the other cellular components of peripheral nerves, axons appear to be disorganized in the neuroma with large regions that lack NF⁺ axons (Figure 1(d), panel c). In contrast, β-tubulin 3 (TUJ1), a marker of new, immature, postmitotic neurons, although present to a small degree in the normal nerve, was not only expressed in a significantly greater numbers of cells in the neuroma but also was more cell associated (Figure 1(d)), suggesting that

there is damage to the pre-existing axons that are being repaired.

Expansion of the cellular component of peripheral nerves in neuroma formation

To quantify the expansion of Schwann cells, flow cytometry for the ErbB2 marker was performed on isolated sciatic nerve segments. There was an approximate two-fold increase in number of ErbB2⁺ cells in the neuroma compared to the uninjured nerve (p = 0.0221) (Figure 2(a)). ADRβ3⁺ cells were quantified using a similar method (Figure 2(b)) and the results show an approximate three-fold increase in the number of ADRβ3⁺ cells within the neuroma as compared to the control nerve (Figure 2(b), p = 0.0009). Since perineurial cells play a key functional role in the regulation of the BNB, the permeability of this barrier was next measured using Evan's blue dye (Figure 2(c)). Sciatic nerves were isolated at 10 days with injection of Evan's blue dye 1 h prior to nerve isolation. Opening of the BNB was visible at day 10 in the neuroma, with a significant difference in permeability of the dye compared to the control nerve (p = 0.0018) (Figure 2(c)).

Targeted suppression of neuroinflammation

To determine if blocking activation of ADRβ3 leads to suppression of perineurial cell expansion, rats received the selective antagonist (L-748,337) daily throughout the period of neuroma formation. Neuromas were isolated from the rats 10 days after initial induction and representative images are shown (Figure 3(a)). To quantify whether the drug was able to suppress perineurial cell expansion, neuromas were isolated and subjected to flow cytometry. ADRβ3⁺ cells were quantified in the resulting neuromas and compared to those receiving vehicle (Figure 3(b)). ADRβ3⁺ cells were six-fold lower in the presence of L-748,337 as compared to vehicle-treated neuroma, which was a statistically significant change (p < 0.001). Alternatively, the number of ADRβ3⁺ was not statistically different from the control nerve. To assess whether Schwann cell replication was suppressed in the presence of the ADRβ3 inhibitor, cells were isolated from the neuromas and quantified by flow cytometry for the presence of ErbB2 (Figure 3(c)). Although there was a trend toward an increase in Schwann cells during neuroma formation in this larger study, it was not statistically significant. Furthermore, there was no statistical difference between the vehicle- and L-748,337-treated groups. The data correlate with the small amount of replicating EGR2⁺ cells observed in Figure 1(c).

Next, a compound that might interfere with the early stages of neuroinflammation was tested. Cromolyn is a compound that blocks mast cell degranulation, one of
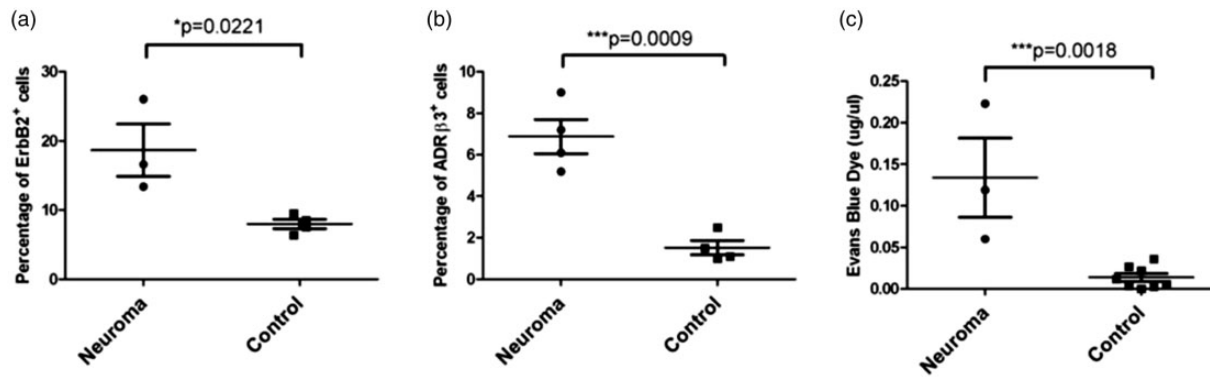
Figure 2. Quantification of changes in Perineurial and Schwann cells during neuroma formation using flow cytometry. (a) Changes in Schwann cells were measured by flow cytometry through immunostaining for ErbB2 or (b) immunostaining for ADRβ3. (c) Blood–nerve barrier permeability was quantified using Evan's blue dye. Data are depicted as µg/µl based on a standard concentration curve for the dye. For all graphs, individual data points are shown on the graph, and horizontal bars represent the average of the data. Error bars depict the standard error of the mean. EGR2: early growth response protein 2; H&E: hematoxylin and eosin; TUJ1: β-tubulin 3.

the earliest steps in the neuroinflammatory cascade. Neuroma formation was established in rats in the presence of cromolyn, and the resultant number of ADRβ3$^+$ cells (Figure 3(b)) and ErbB2$^+$ cells (Figure 3(c)) were quantified and compared to vehicle-treated control. Cromolyn was able to suppress the neuroma as indicated both by gross observation (Figure 3(a)) and a histological analysis of the two cellular components of the nerve (Figure 3(b) and (c)). ADRβ3$^+$ cells were three-fold less as compared to the vehicle-treated control, but this was not statistically different from the control nerve (Figure 3(b) and (c)). Neither were ErbB2$^+$ cells decreased in the presence of cromolyn.

Finally, to confirm whether these compounds could influence the status of the BNB, Evan's blue dye was delivered to a set of rats exposed to cromolyn, L-748,337, or saline and compared to the normal sciatic nerve of approximately the same length. The data suggest that the drugs showed a trend toward retaining BNB regulation (Figure 3(d)). Although there seemed to be a trend toward differences between chromic gut treated, saline, and normal nerve, there was no statistical difference between the treatment groups.

## Suppression of neuroma results in functional improvement

Since cromolyn and L-748,337 treatments appeared to be able to reduce the size of the neuroma, experiments were performed to measure the improvement in limb function, which could also depict neuroma-related pain. To assess these changes, the CatWalk system was used to measure various parameters including, stance, swing, intensity, contact area, and deviation in the run. Mice were first run prior to surgery (day 0) to provide a baseline and then 5 and 10 days later (Figure 4). In all

cases, there was an increase in limb swing (Figure 4(a)) and step cycle (Figure 4(b)) after introduction of the chromic gut sutures, indicating pain and altered limb function. With all treatments, limb swing was significantly increased over the pre-operative values, independent of the drug treatment. Whereas in step cycle, delivery of the ADRβ3 antagonist appeared to resolve to pre-operative values by day 10. Furthermore, comparison between the groups of mice receiving saline or the two compounds showed a statistically significant improvement in these measured parameters (Figure 4 (a) and (b)) on day 5.

Limb stand or the length of time the mouse has contact with the surface and maximum contact maximum intensity were also both analyzed 5 and 10 days after surgery for the left hind limb or the limb that received the chromic gut suture. There was a statistically significant decrease in the time the limb contacted the surface (stand) in all groups following surgery, regardless of timing of the measurements. However, there was a small but significant improvement observed in the group receiving L-748,337 as compared to the saline group on day 10. Although the cromolyn appeared to be trending higher, suggesting improvement, there was no significant difference. The final parameter analyzed for the limb possessing the chromic gut suture, was maximum contact/maximum intensity. Again, in all cases after surgery, the values decreased significantly compared to the preoperative values. However, there was a statistically significant (p < 0.05) difference in comparisons made between the day 5 and day 10 values for the cromolyn and L-748,337 groups, which was not seen in the saline group. Furthermore, on day 10, there was a statistically significant increase in the group receiving the ADRβ3 antagonist as compared to the saline group, which suggests a significant improvement. Again, the
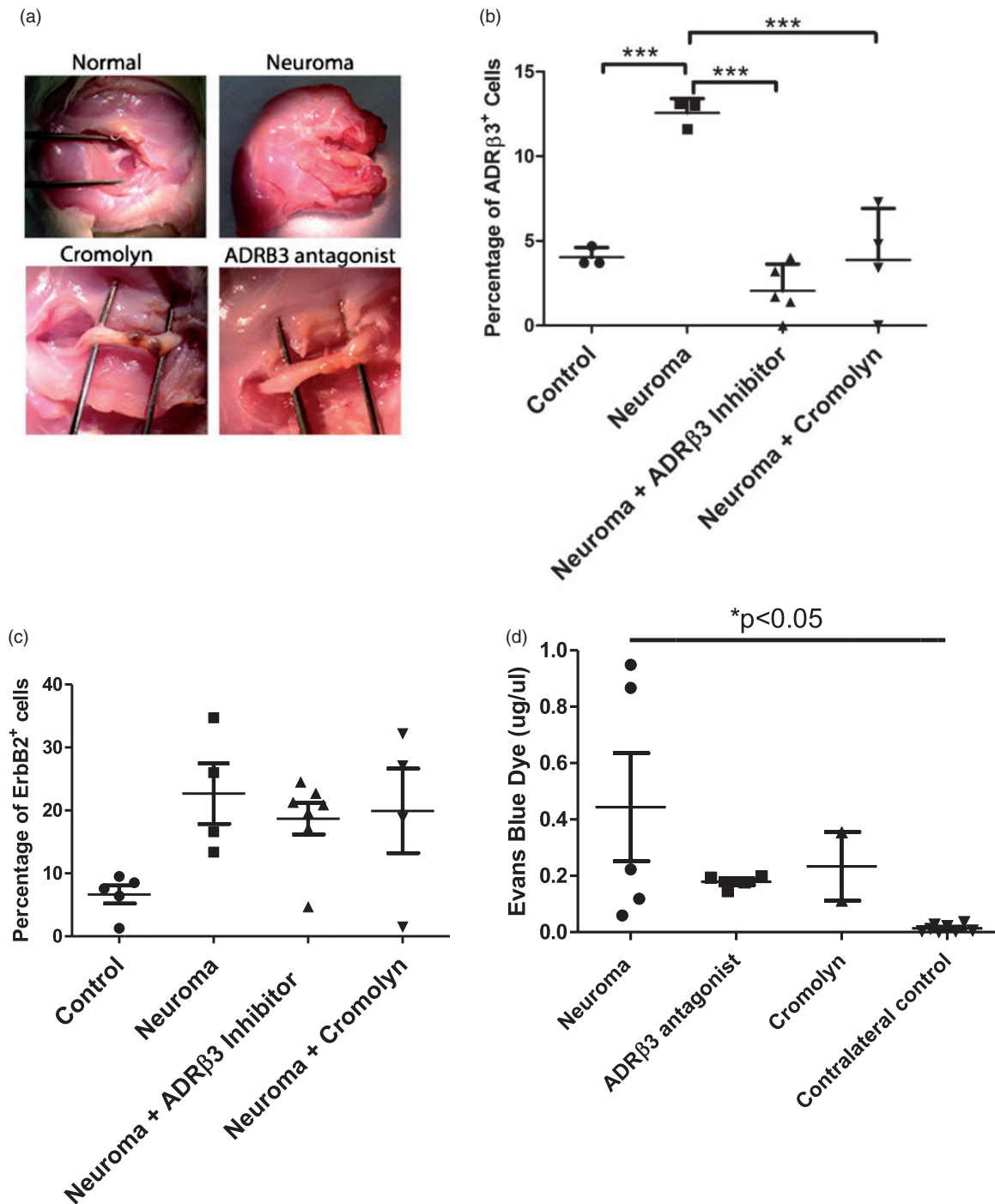
Figure 3. (a) Representative photographs of resultant rat sciatic nerve neuromas in the presence of either cromolyn or ADRβ3 antagonist as indicated. Both the normal sham-operated nerve (Normal) and neuroma that received the vehicle control (saline) (Neuroma) are shown. Quantification of (b) perineurial (ADRβ3⁺) cells and (c) Schwann (ErbB2⁺) cells from groups described in (a). (d) Blood–nerve barrier permeability was quantified using Evan's blue dye 10 days after induction of neuroma. Resultant data points are depicted on the graph, and horizontal bars represent the average of the group. Error bars depict the standard error of the mean. Statistical significance is shown when present (c) ***$p < 0.001$ and (d) *$p < 0.05$. ADRβ3: beta-3 adrenergic receptor.
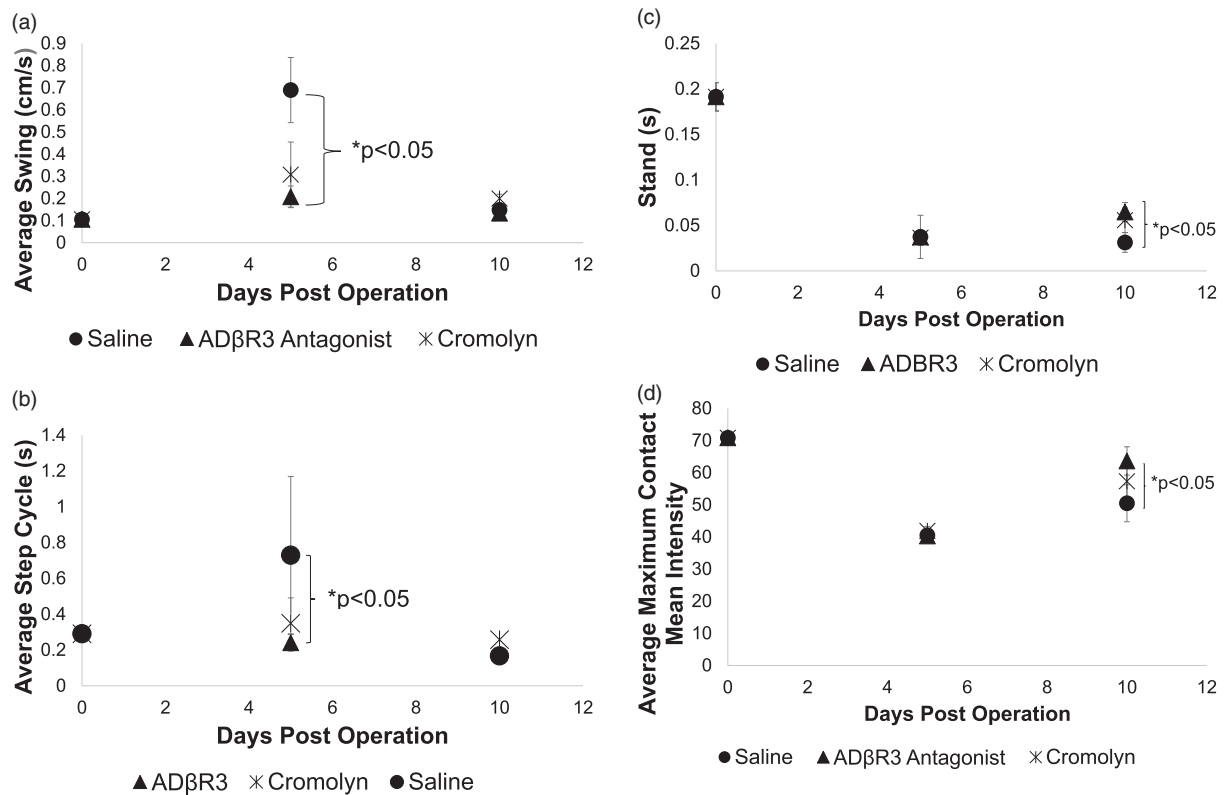
Figure 4. Quantification of (a) limb swing, (b) step cycle, (c) stand, and (d) maximum contact/maximum intensity of the left hind limb. Mice were initially run on the catwalk system, and values were recorded. These pre-operative values are shown on the graph as day 0. Mice then underwent surgery where chromic gut sutures were loosely ligated around the left limb sciatic nerve to induce neuroma. The mice were rerun on the catwalk system 5 and 10 days post-surgery. Values for the left hind limb possessing the neuroma were used for analysis. Symbols depict the mean for each group. Error bars depict the standard error of the mean, and statistical significance was calculated between groups using a one way analysis of variance with a Tukey correction. (a and b) Statistical significance is shown between the L-748,337 and saline groups on day 5 (bracket) or (c and d) day 10 (bracket). The graph does not show (a) the comparison of pre-operative and day 10 values resulted in saline and cromolyn-treated groups being highly statistically significant (p < 0.001) and L-748,337-treated group being statistically different (p < 0.05) for limb swing. (b) Comparisons between pre-operative and day 10 values for step cycle showed a significant difference only in the saline and cromolyn-treated groups (p < 0.001). The ADRβ3 antagonist group was not statistically different from the pre-operative values. (c and d) Comparison between the pre-operative and day 10 values per group were significantly different (p < 0.001). ADRβ3: beta-3 adrenergic receptor.

cromolyn group values appeared to trend higher than the saline group on day 10, but this difference was not significant.

Effects of HO on neuroma

To determine potential interactions between neuroma and HO, these two processes were induced simultaneously in the same limbs. Approximately 10 days after induction, the resultant bone formation and neuroma formation were analyzed and the groups compared to one another. Flow cytometry quantification showed changes in the number of Schwann cells (ErbB2$^+$) with a trend toward decreasing numbers when HO was present in the limb, but this was not statistically significant (Figure 5(a)). Comparisons between these same groups for ADRβ3$^+$ cells showed a statistically significant

decrease (p = 0.0256) in the limbs undergoing both HO and neuroma as compared to the neuroma group alone (Figure 5(b)).

Alternatively, the analysis of heterotopic bone formation was surprising in that neuroma appeared to enhance the volume of bone formed (p < 0.05) as compared to the HO group alone (Figure 5(c)). Bone mineral density was also calculated, and it correlates with the maturity of the heterotopic bone. There was no statistical difference in bone mineral density (Figure 5(d)).

Discussion

In these studies, loose ligation of chromic gut suture was used to induce neuroma formation. We observed neuroma formation in approximately 90% to 95% of the animals, either rats or mice. This was the only neuroma
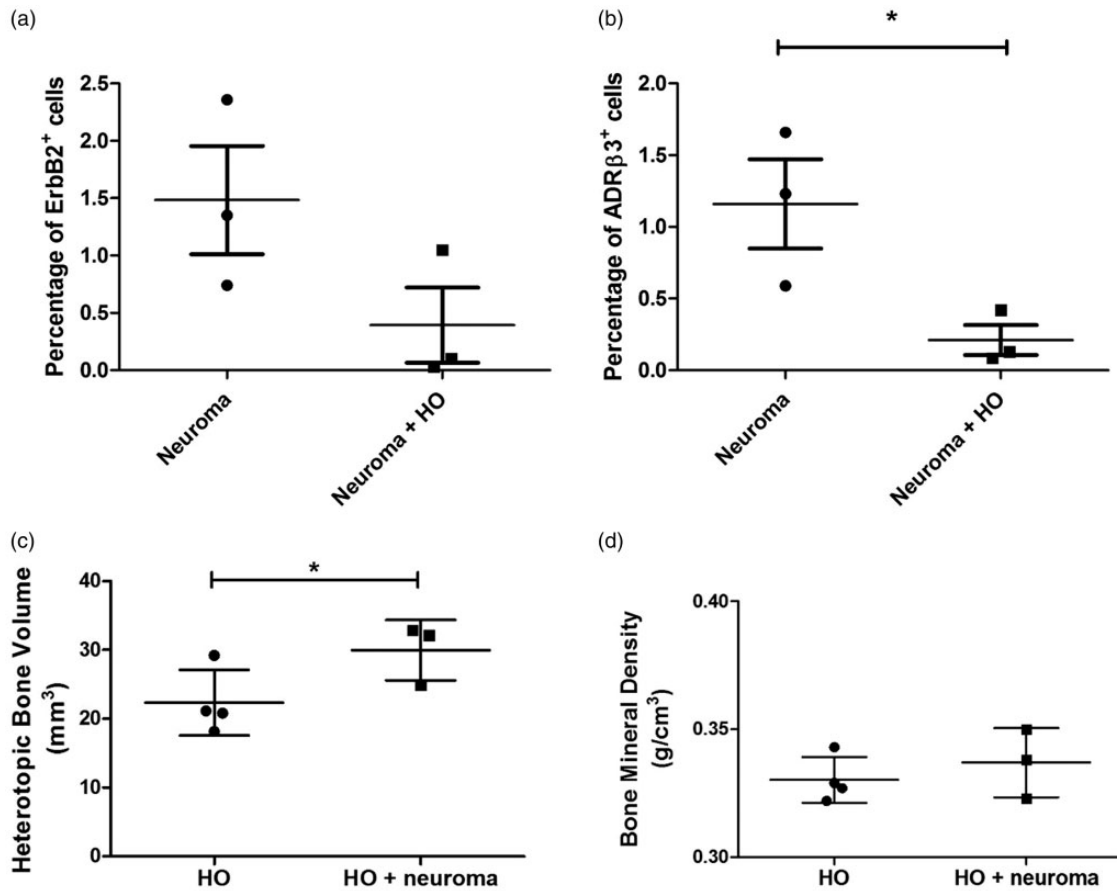
Figure 5. Quantification of (a) Schwann and (b) perineurial cells in mouse sciatic nerve from mice receiving 5×10^6 AdBMP2 transduced cells to induce HO, loose ligation of chromic gut sutures 3 mm apart (neuroma), or mice receiving the AdBMP2 transduced cells simultaneous with introduction of the chromic gut sutures (HO + neuroma). Quantification of (c) bone volume and (d) bone mineral density of heterotopic ossification in mice. Groups consist of mice receiving 5×10^6 AdBMP2 transduced cells to induce HO alone, or in the same hind limb simultaneously receiving loose ligation of chromic gut sutures (HO + neuroma). Heterotopic bone was quantified using a threshold value of 45, which is below the normal threshold for skeletal bone, since the heterotopic bone during this time frame has not yet undergone remodeling. For all graphs, individual data points are shown on the graph, and horizontal bar represents the average of the data. Error bars depict the standard error of the mean, and statistical significance was calculated between the two groups using a one-way analysis of variance with a Tukey post hoc test. Statistical significance and p-values are shown. HO: heterotopic ossification.

model tested that would reliably lead to neuromas in these rodent models. Although stretch injury of the sciatic nerve resulted in neuroma approximately 30% of the time, crush injury or transection did not result in the formation of neuroma. Animals undergoing neuroma formation exhibited pain and were provided continuous analgesia. However, approximately 15% of the animals had break-through pain, which could not be alleviated, that led to autophagy of their limbs, requiring early euthanasia. In these cases, neuromas could not be macroscopically appreciated, suggesting that exposure to the chromic gut sutures caused significant neuroinflammation and pain without evidence of neuroma. All cases of animals terminated prematurely were excluded from the studies. In all term cases, neuromas were analyzed at 10 days.

Histological analysis of the resultant neuromas suggested a disorganized region in the sciatic nerve that appeared to have both replicating Schwann (EGR2^{+} Ki-67^{+}) and perineurial (ADRβ3[+] Ki-67^{+}) cells. Untreated nerves expressed the Schwann cell marker ErbB2, whereas there was almost a complete absence of ADRβ3 expression in the normal nerve. As noted by flow cytometry, the ADRβ3^{+} perineurial cells were significantly increased in neuroma, while the Schwann cell expansion was more modest. Since disruption of axons leading to extension or arborization is commonly associated with trauma-induced neuromas, changes in the axons were measured through immunohistochemistry using antibodies against NF heavy chain, which is highly expressed in mature axons, and β-Tubulin 3 (TUJ1), which is found in sprouting axons. The control

nerve had minor expression of TUJ1, and NF+ axons were distributed in an organized manner throughout the entire nerve. Alternatively, in the neuroma, TUJ1 expression was more robust, and the organized NF$^+$ axons were absent, suggesting that like trauma-induced neuromas, the axons were disrupted and appeared to be attempting to regenerate.

Analysis of the BNB showed that this structure was opened early on in the process of neuroma formation and remained open, presumably due to the disorganized expansion of the perineurial cells. The data collectively suggest that during neuroma expansion, the cellular component (perineurial and Schwann cells) of the nerve expands leading to disruption of the BNB. This allows inflammatory cells to enter, which would contribute to pain. Furthermore, the immediate opening would potentially lead to chronic release of pain mediators, and allodynia, which might explain the loss of animals from the study due to self-mutilation. In addition, axons become damaged, disconnected, or disorganized, leading to what appears to be a repair process.

Thus, potential suppression of either neuroinflammation, or directly blocking cellular expansion, may allow the BNB to remain intact and prevent formation of the painful neuroma. To this end, two compounds were employed: one that selectively targeted ADRβ3, which should prevent the proliferation of perineurial cells essential to the BNB, and cromolyn.[12] Delivery of cromolyn and the ADRβ3 antagonist throughout the period of neuroma formation appeared to stabilize the BNB and prevent the significant changes in permeability as indicated by the statistically significant difference in Evan's blue dye uptake compared to the group receiving saline.

Flow cytometric analysis of the cells associated with the nerve after cromolyn treatment and comparisons to the saline-treated group showed a statistically significant decrease in cell number (ADRβ3$^+$ perineurial) in the presence of either drug, whereas the ErbB2+ (Schwann) cell appeared unchanged. This may be due in part to the fact that there was only a modest increase in these cells upon neuroma formation and that the tumor itself appeared to arise from the changes in perineurial cells. A further problem was that although neuromas would reliably form, the volume of the final neuroma was highly variable. Thus, since the volume of neuroma could not be controlled in these studies, a large variability or standard error is observed in these groups, potentially obscuring small changes.

We next attempted to analyze whether these compounds could prevent or suppress neuroma formation and alleviate pain, permitting restoration of limb function. The Catwalk system was used to measure a number of parameters collectively depicting the animal's gait and neuroma-related pain. An increase in step cycle and

swing with a decrease in stand and maximum contact and intensity in values obtained from measuring the limb involved in neuroma formation is an indication of pain. All animals regardless of drug treatment had a statistically significant difference in these parameters, when comparing pre-operative to day 10 values, with the exception of the swing parameter where the group receiving L-748,337 day 10 values were not statistically different from pre-operative. However, in all cases, this same group appeared to be statistically different from saline on either day 5 or day 10, suggesting that this group was able to potentially improve the pain associated with use of the limb. Cromolyn also appeared to improve limb function but to a lesser degree. Although the improvement in pain may suggest analgesic benefit, antagonists of the ADRβ3 receptor have not been associated with suppression of pain mediators. Furthermore, the data collectively suggest that the ADRβ3 antagonist appeared to suppress expansion of the perineurial cells. The data suggest that blocking expansion of these cells may better maintain the BNB and also suppress the formation of the neuroma.

To determine if neuroma could influence HO formation, both processes were introduced into mice. Perineurial cells and Schwann cells were isolated from sciatic nerves isolated from limbs undergoing neuroma or neuroma and HO. Comparisons were made between the resultant neuroma/HO in these mice and mice undergoing either neuroma formation or HO alone. The results suggest that the presence of HO appeared to significantly decrease the number of perineurial cells suggesting a decrease in neuroma formation as compared to the neuroma alone group. Alternatively, the presence of neuromas appeared to increase HO bone volume significantly. This suggests that disruption of the BNB and the expansion and mobilization of perineurial cells during neuroma formation may enhance HO in mice.

Previous studies involving HO suggest that these perineurial cells expand and migrate to support HO.[15] The studies presented here suggest that during neuroma formation, these cells also expand but they do not migrate. Thus, the significant increase in HO volume in the presence of neuroma may be due in part to the neuroma and HO both providing inductive components, which lead to perineurial cell proliferation. However, since HO also induces migration, this may in part explain why the neuromas were actually smaller in the limbs which were undergoing HO. Perhaps neuromas, that are a disorganized expansion of the nerve components, may be reduced when these components are recruited toward the HO. If neuroma, which also mobilizes perineurial cells, is able to do this rapidly, that may ultimately impact bone remodeling leading to the slight elevation observed in bone mineral content. Thus, HO may induce migration of these cells, removing them from peripheral

nerve, preventing the disorganization and disruption of axons, and potentially permitting the BNB to remain closed, while expanding the volume of bone formation.

The data collectively suggest that the ADRβ3 antagonist L-748,337, and to a lesser extent cromolyn, may provide benefit to suppressing neuroma formation, and restoring limb function. Furthermore, the data suggest that neuroma formation and HO are not exclusive events but can impact each other when present in the same limb.

Acknowledgments

Author Contributions

JM was involved in conception and design, collection and assembly of data, data analysis and interpretation, and manuscript writing; ELD was involved in conception and design, data analysis and interpretation, and manuscript preparation; AD, WCM, and JAM contributed to collection and assembly of data; ZG was involved in microCT analysis and interpretation, conception and design, and analysis and interpretation of data; and ARD and EAOD contributed to conception and design, data analysis and interpretation, administrative support, manuscript writing, and final approval of the manuscript.

Declaration of Conflicting Interests

Funding

References

1. Maves TJ, Pechman PS, Gebhart GF and Meller ST. Possible chemical contribution from chromic gut sutures produces disorders of pain sensation like those seen in man. *Pain* 1993; 54: 57–69.

2. Jeon SM, Lee JY and Byeon SJ. Traumatic neuroma at the inferior mesenteric artery stump after rectal cancer surgery: a case report and literature review. *Korean J Gastroenterol* 2016; 68: 279–283.

3. Baron R, Maier C, Attal N, Binder A, Bouhassira D, Cruccu G, Finnerup NB, Haanpää M, Hansson P, Hüllemann P, Jensen TS, Freynhagen R, Kennedy JD, Magerl W, Mainka T, Reimer M, Rice AS, Segerdahl M, Serra J, Sindrup S, Sommer C, Tölle T, Vollert J and Treede RD. Peripheral neuropathic pain: a mechanism-related organizing principle based on sensory profiles. *Pain* 2017; 158: 261–272.

4. Morton TG. A peculiar and painful affection of the fourth metatarsophalangeal articulation. *Am J Med Sci* 1876; 71: 37–45.

5. Goldman F. Intermetatarsal neuroma: light microscopic observations. *J Am Podiatry Assoc* 1979; 69: 317–324.

6. Goldman F. Intermetatarsal neuromas: light and electron microscopic observation. *J Am Podiatry Assoc* 1980; 70: 265–278.

7. Hsu E and Cohen SP. Postamputation pain: epidemiology, mechanisms, and treatment. *J Pain Res* 2013; 6: 121–136.

8. Sehirlioglu A, Ozturk C, Yazicioglu K, Tugcu I, Yilmaz B and Goktepe AS. Painful neuroma requiring surgical excision after lower limb amputation caused by landmine explosions. *International Orthopaedics (Sicot)* 2009; 33: 533–536.

9. Kang J, Yang P, Zang Q and He X. Traumatic neuroma of the superficial peroneal nerve in a patient: a case report and review of the literature. *World J Surg Oncol* 2016; 14: 242.

10. Dworkin RH, O'Connor AB, Audette J, Baron R, Gourlay GK, Haanpää ML, Kent JL, Krane EJ, Lebel AA, Levy RM, Mackey SC, Mayer J, Miaskowski C, Raja SN, Rice AS, Schmader KE, Stacey B, Stanos S, Treede RD, Turk DC, Walco GA and Wells CD. Recommendations for the pharmacological management of neuropathic pain: an overview and literature update. *Mayo Clin Proc* 2010; 85: S3–S14.

11. Salisbury E, Sonnet C, Heggeness M, Davis AR and Olmsted-Davis E. Heterotopic ossification has some nerve. *Crit Rev Eukaryot Gene Expr* 2010; 20: 313–324.

12. Salisbury E, Rodenberg E, Sonnet C, Hipp J, Gannon FH, Vadakkan TJ, Dickinson ME, Olmsted-Davis EA and Davis AR. Sensory nerve induced inflammation contributes to heterotopic ossification. *J Cell Biochem* 2011; 112: 2748–2758.

13. Kan L, Lounev VY, Pignolo RJ, Duan L, Liu Y, Stock SR, McGuire TL, Lu B, Gerard NP, Shore EM, Kaplan FS and Kessler JA. Substance P signaling mediates BMP-dependent heterotopic ossification. *J Cell Biochem* 2011; 112: 2759–2772.

14. Zhao B-Q, Tejima E and Lo EH. Neurovascular proteases in brain injury, hemorrhage and remodeling after stroke. *Stroke* 2007; 38: 748–752.

15. Salisbury EA, Lazard ZW, Ubogu EE, Davis AR and Olmsted-Davis EA. Transient brown adipocyte-like cells derive from peripheral nerve progenitors in response to bone morphogenetic protein 2. Stem Cells. *Transl Med.* 2012; 1: 874–885.

16. Beggs S, Liu XJ, Kwan C and Salter MW. Peripheral nerve injury and TRPV1-expressing primary afferent C-fibers cause opening of the blood-brain barrier. *Mol Pain* 2010; 6: 74.

17. Olmsted-Davis EA, Gugala Z, Gannon FH, Yotnda P, McAlhany RE, Lindsey RW and Davis AR. Use of a chimeric adenovirus vector enhances BMP2 production and bone formation. *Hum Gene Ther* 2002; 13: 1337–1347.

18. Fouletier-Dilling CM, Gannon FH, Olmsted-Davis EA, Lazard Z, Heggeness MH, Shafer JA, Hipp JA and Davis AR. Efficient and rapid osteoinduction in an immune-competent host. *Hum Gene Ther* 2007; 18: 733–745.
19. Batka RJ, Brown TJ, Mcmillan KP, Meadows RM, Jones KJ and Haulcomb MM. The need for speed in rodent locomotion analyses. *Anat Rec* 2014; 297: 1839–1864.
20. Olmsted-Davis E, Gannon FH, Ozen M, Ittmann MM, Gugala Z, Hipp JA, Moran KM, Fouletier-Dilling CM, Schumara-Martin S, Lindsey RW, Heggeness MH, Brenner MK and Davis AR. Hypoxic adipocytes pattern early heterotopic bone formation. *Am J Pathol* 2007; 170: 620–632.